



# Evaluation of magnetic nanoparticles to serve as solid-phase extraction sorbents for the determination of endocrine disruptors in milk samples by gas chromatography mass spectrometry



Maria-Evangelia S. Synaridou<sup>1</sup>, Vasilios A. Sakkas\*, Constantine D. Stalikas<sup>2</sup>, Triantafyllos A. Albanis<sup>3</sup>

Laboratory of Analytical Chemistry, Department of Chemistry, University of Ioannina, Ioannina 45110, Greece

## ARTICLE INFO

### Article history:

Received 12 February 2014

Received in revised form 10 April 2014

Accepted 26 April 2014

Available online 2 May 2014

### Keywords:

Magnetic solid-phase extraction

Magnetite octadecylsilane nanoparticles

Milk

Organochlorine pesticides

Polychlorinated biphenyls

Experimental design

## ABSTRACT

A rapid magnetic solid-phase extraction (MSPE) is proposed based on C18-functionalized magnetic silica nanoparticles as sorbents, for the determination of endocrine disruptors – 20 organochlorine pesticides and 6 polychlorinated biphenyls – in milk samples. Magnetic nanoparticles are characterized by several techniques, such as Scanning Electron Microscopy, X-Ray diffraction, Brunauer–Emmett–Teller and Fourier transform-infrared. The MSPE is performed by dispersion of the Fe<sub>3</sub>O<sub>4</sub>@SiO<sub>2</sub>@C18 nanoparticles in milk samples with sonication, after protein precipitation. Then, the sorbent is collected by applying an external magnetic field and the analytes are desorbed by *n*-hexane. Several parameters affecting the extraction efficiency of target analytes by the magnetic nanoparticles are investigated, including washing and elution solvents, amount of sorbents, time of extraction and elution, sample and elution solvent volume. The proposed method is optimized by means of experimental design and response surface methodology. When coupled with gas chromatography–mass spectrometry detection and under optimum extraction conditions, average recoveries of target analytes are found to be in the range of 79% to 116%. The proposed MSPE–GC–MS analytical method has a linear calibration curve for all target analytes with coefficients of determination to range from 0.9950 to 0.9999. The limits of quantification are found to be between 0.2 and 1 µg/L ensuring compliance with the maximum residue limits established by European Commission and Codex Alimentarius, for OCPs and PCBs residues in milk. The proposed method is applied to the determination of target analytes in milk samples from local markets.

© 2014 Elsevier B.V. All rights reserved.

## 1. Introduction

Exposure to endocrine disruption chemicals (EDCs) has become lately a predominant issue in environmental science research and policy, receiving increased public attention. Recently, the U.S. EPA released a much anticipated draft list of compounds to screen for endocrine disruption [1]. The EDCs refer to those compounds that can mimic or block the actions of natural hormones in living organisms and impair their normal functioning, such as growth, metabolism and reproduction [2]. European Commission has also

published a draft list of chemicals, which are believed to damage health by interfering with the way hormones work [3–5].

Organochlorine pesticides (OCPs) have been extensively used as pesticides in agriculture, while polychlorinated biphenyls (PCBs) have been employed as industrial fluids mainly in transformers, capacitors, papers and paints industry. Both groups of compounds are highly lipophilic, chemically stable and resistant to environmental degradation, while they are included in relevant lists, as having potential or suspected endocrine activity. However, although these chemicals were banned more than 30 years ago and no longer used, they are globally spread into the environment and may be routinely detected in surface waters, air, fish, wildlife, food and even humans [2,6–12].

Cow's milk is a major constituent of the daily diet, principally for vulnerable groups such as infants, school age children and elderly. Due to their lipophilic properties, OCPs and PCBs are primarily stored in fat-rich tissues [13] and subsequently translocated and excreted through milk fat [14]. Thus, knowledge of cow's milk

\* Corresponding author. Tel.: +30 26510 08303; fax: +30 26510 08796.

E-mail addresses: [msynarid@cc.uoi.gr](mailto:msynarid@cc.uoi.gr) (M.-E.S. Synaridou), [vsakkas@cc.uoi.gr](mailto:vsakkas@cc.uoi.gr) (V.A. Sakkas), [cstalika@cc.uoi.gr](mailto:cstalika@cc.uoi.gr) (C.D. Stalikas), [talbanis@cc.uoi.gr](mailto:talbanis@cc.uoi.gr) (T.A. Albanis).

<sup>1</sup> Tel: +30 26510 08399.

<sup>2</sup> Tel: +30 26510 08414.

<sup>3</sup> Tel: +30 26510 08363.

contamination by EDCs provides important information about human exposure to these contaminants, through the consumption of dairy products. One of the main difficulties related to the determination of these analytes in milk samples, is the high protein and fat content that can often interfere during the analytical determination. For this reason, sample pretreatment and/or extraction can be long and tedious, involving several clean-up steps to remove the co-extracted material from the matrix [15,16].

Several methodologies [15] have been reported for the determination of PCBs and OCPs from cow milk samples, such as solid-phase microextraction (SPME) [17], dispersive solid-phase extraction (DSPE) [18], QuEChERS (quick, easy, cheap, effective, robust and safe) [19] and liquid–liquid extraction (LLE) [20–22]. Solid-phase extraction (SPE) is also widely used for the extraction and/or clean-up of milk samples, since it offers an excellent alternative to conventional sample preparation techniques, such as LLE, because of its simplicity, flexibility to choose the sorbents, low consumption of environmental and health hazardous organic solvents as well as due to the ability to achieve high preconcentration factors [14,23–26].

Magnetic solid-phase extraction (MSPE), which has drawn extensive attention in sample preparation in recent years, is a new mode of SPE based on the adoption of magnetic nanoparticles (MNPs) as sorbents, at micro- or nano-scale and shows great advantages in separation science. The powdery magnetic adsorbent can be reversibly agglomerated and re-dispersed in solution or suspensions by the application and removal of an appropriate magnetic field, thus realizing the phase separation conveniently [27,28].

In this article, we describe the chemometric optimization and validation of a simple and rapid method based on MSPE, which is followed by gas chromatography coupled with mass spectrometry for the determination of EDCs in milk samples. Magnetite octadecylsilane nanoparticles ( $\text{Fe}_3\text{O}_4@\text{SiO}_2@\text{C18}$ ) are synthesized by coating magnetite  $\text{Fe}_3\text{O}_4$  nanoparticles with silica and subsequently functionalizing it by trimethoxy(octadecyl)silane. The resultant MNPs are characterized by several techniques, such as scanning electron microscopy (SEM), X-ray diffraction (XRD), Elemental Analysis (EA), Fourier transform-infrared (FT-IR) and Brunauer–Emmett–Teller (BET).

## 2. Experimental

### 2.1. Chemicals and materials

All the chemicals and reagents used were of analytical grade. Aldrin, endrin, dieldrin,  $\alpha$ -BHC,  $\beta$ -BHC,  $\gamma$ -BHC,  $\delta$ -BHC,  $\alpha$ -chlordane,  $\gamma$ -chlordane,  $p,p'$ -DDE,  $p,p'$ -DDT,  $p,p'$ -DDD, endosulfan I, endosulfan II, endosulfan sulfate, endrin aldehyde, heptachlor, heptachlor epoxide, endrin ketone and methoxychlor were purchased from Sigma-Aldrich Chemie (Steinheim, Germany). PCBs standards (PCB 28, 52, 101, 138, 153 and 180) were obtained from Fluka (Milwaukee, WI, USA). A mixture containing the investigated compounds at concentrations of 300  $\mu\text{g}/\text{mL}$ , in isoctane was prepared and used as working solution.

Ferric chloride ( $\text{FeCl}_3$ ) was purchased from Fluka (Milwaukee, WI, USA) and ferrous chloride tetrahydrate ( $\text{FeCl}_2 \cdot 4\text{H}_2\text{O}$ ) from Ferak (Berlin, Germany). Tetraethyl orthosilicate (TEOS) and trimethoxy(octadecyl)silane (99%) were purchased from Aldrich. Formic acid and ammonia were obtained from Merck (Darmstadt, Germany). Carrez 1 solution was prepared by dissolving 1.5 g of potassium hexacyanoferrate(II) trihydrate (Sigma-Aldrich) in 10.0 mL of water, and Carrez 2 solution was prepared by dissolving 3.0 g of zinc sulfate heptahydrate (Sigma-Aldrich) in 10.0 mL of water. All solvents used were of pesticide residue analysis grade

and purchased from Labscan (Dublin, Ireland). Membrane filters (PVDF, 0.45  $\mu\text{m}$ ) were obtained from Millipore (Ireland).

### 2.2. Samples and sample preparation

Initially, method optimization and validation experiments were performed with a biological semi-skimmed milk sample (fat content <1.5% w/w), purchased from local market and was found to be satisfactory as a blank for the target analytes. Milk samples were kept at 4 °C, until use.

### 2.3. Apparatus

Chromatographic analysis of OCPs and PCBs was performed using a Trace GC Ultra instrument (Thermo Scientific, Waltham, MA, USA) coupled to an ISQ mass spectrometer controlled by a computer running X-Calibur software. Aliquots of 1  $\mu\text{L}$  were injected using an AI/AS 3000 auto sampler (Thermo Scientific). The separation was performed using a SLB fused silica column 30 mm  $\times$  0.25 mm i.d., with film thickness of 0.25 mm (Supelco, Bellefonte, PA, USA). Helium was the carrier gas at a constant inlet flow rate of 1.5 mL/min (constant flow). The GC oven temperature program was as follows: initial temperature 60 °C held for 5 min, ramped at 8 °C/min to 300 °C (held for 2 min) (total acquisition time program: 45 min). The ion source and transfer line were kept at 225 and 250 °C, respectively. In the full-scan mode, electron ionization mass spectra at  $m/z$  of 50–500 were recorded at 70 eV. In the selected ion monitoring (SIM) mode acquisition, target ions were monitored at different time windows defined by the corresponding retention times. Three diagnostic ions were chosen for each analyte, according to the mass spectra characteristics obtained in the full-scan mode as well as by comparison with NIST library. The quality criteria used were the following: the relative retention time of the analytes, corresponded to that of the matrix-matched calibration solution with a tolerance of  $\pm 0.5\%$  and the relative intensities of the selected ions did not differ more than 10% from the relative intensities of the same ions acquired from a spiked sample.

The SEM images, after gold coating were taken by a JOEL microscope (JSM-5600, JEOL, Tokyo, Japan) to assess the morphology of MNPs.

To characterize the functionalized MNPs and ensure their proper fabrication, FT-IR spectroscopy (FTIR, Perkin Elmer, spectrum 100, Waltham, MA, USA) was employed. In addition, elemental analysis of  $\text{Fe}_3\text{O}_4@\text{SiO}_2@\text{C18}$  NPs was performed on a Vario Macro CNS (Elemental Analyzensysteme GmbH, Hanau, Germany).

The surface area of MNPs was calculated based on  $\text{N}_2$  adsorption–desorption porosimetry according to the BET method on an Autosorb-1 porosimeter (QUANDACHROM, Bounton Beach, FL, USA). Before measurement, the sample was degassed at 80 °C, for 5 h.

Finally, the crystal phases of  $\text{Fe}_3\text{O}_4$ ,  $\text{Fe}_3\text{O}_4@\text{SiO}_2$  and  $\text{Fe}_3\text{O}_4@\text{SiO}_2@\text{C18}$  MNPs were investigated by X-ray diffraction, using a D8 Advance Brüker diffractometer operating with  $\text{Cu K}\alpha$  ( $\lambda = 1.5406 \text{ \AA}$ ) radiation and a secondary beam graphite monochromator. Powder samples were scanned over an angular  $2\theta$  range from 10 to 90°, in steps of 0.02° ( $2\theta$ ), at a rate of 2 s per step.

### 2.4. Preparation of magnetite octadecylsilane nanoparticles

#### 2.4.1. Synthesis of magnetite ( $\text{Fe}_3\text{O}_4$ ) nanoparticles

The nanoparticles of  $\text{Fe}_3\text{O}_4$  were synthesized by coprecipitation of  $\text{Fe}^{2+}$  and  $\text{Fe}^{3+}$  ions, at alkaline conditions and under hydrothermal treatment [29,30]. Briefly, 0.7 g of  $\text{FeCl}_3$  and 0.42 g of  $\text{FeCl}_2 \cdot 4\text{H}_2\text{O}$  were dissolved in 100 mL deionized water, degassed continuously with  $\text{N}_2$  to agitate the mixture and prevent

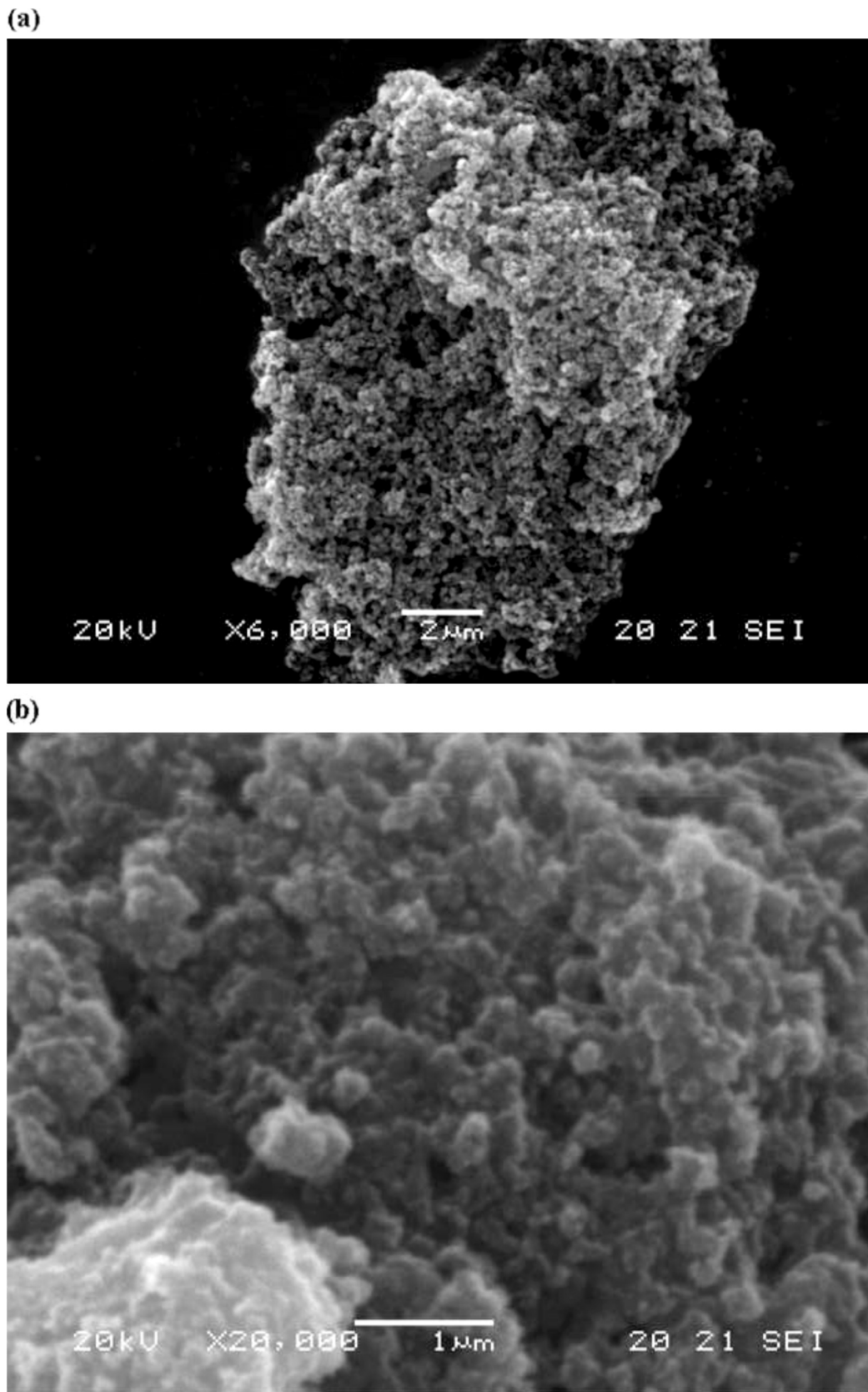


Fig. 1. SEM images of (a)  $\text{Fe}_3\text{O}_4@SiO_2$  and (b)  $\text{Fe}_3\text{O}_4@SiO_2@C18$ .

the oxidation of  $\text{Fe}^{2+}$  ions. After 10 min of intense bubbling, 5 mL of 25% (w/w)  $\text{NH}_3$  were added and the mixture was held at  $80^\circ\text{C}$  in a water bath for 30 min, with vigorous magnetic stirring (5000 rpm). After cooling down to room temperature, the black iron oxide nanoparticles were rinsed several times with deionized water and ethanol.

#### 2.4.2. Fabrication of silica gel-modified magnetic nanocomposites ( $\text{Fe}_3\text{O}_4@SiO_2$ )

$\text{Fe}_3\text{O}_4@SiO_2$  nanoparticles were synthesized by the Stöber process with minor modifications [31–33]. First, 0.5 g  $\text{Fe}_3\text{O}_4$  NPs were dispersed in a mixture containing 12.5 mL ethanol and 4 mL deionized water with the aid of ultrasonication, for 5 min. Then, 250  $\mu\text{L}$  TEOS and 500  $\mu\text{L}$  ammonia 25% (w/w) were added dropwise under vigorous stirring (5000 rpm) in a period of 10 min. The reaction was allowed to proceed for 12 h. Finally, the nanoparticles were rinsed several times with ethanol and dried under vacuum for 24 h thus obtaining a gray–black powder of  $\text{Fe}_3\text{O}_4@SiO_2$  nanocomposites.

#### 2.4.3. Preparation of octadecylsilane nanoparticles ( $\text{Fe}_3\text{O}_4@SiO_2@C18$ )

The C18 was selected as the bonded phase, due to its lipophilic character that enables retention of lipophilic species (such as OCPs and PCBs) while high recoveries can be obtained minimizing the presence of interferences [25]. The C18 alkylchain was efficiently bonded to the surface of magnetite silica nanoparticles through the Si–OH active sites [34]. Initially, 0.2 g silica-coated NPs were dispersed in 70 mL toluene with the aid of ultrasonication. The slurry was heated to boiling and 200  $\mu\text{L}$  of trimethoxy(octadecyl)silane were added under vigorous stirring (5000 rpm). The mixture was then refluxed for 12 h, at  $80^\circ\text{C}$ . After cooling down to room temperature, the black product ( $\text{Fe}_3\text{O}_4@SiO_2@C18$ ) was rinsed with toluene and ethanol several times and dried under vacuum at room temperature, before use.

#### 2.5. Magnetic solid-phase extraction (MSPE) procedure

Three mL of milk sample were diluted with Milli Q water (1:1, v/v), mixed with formic acid (2 mL) and acetonitrile (125  $\mu\text{L}$ ) and equilibrated by ultrasonic treatment, for 15 min [35]. Then, aliquots of Carrez 1 (100  $\mu\text{L}$ ) and Carrez 2 (100  $\mu\text{L}$ ) were added. After gentle mixing for 2 min, the samples were centrifuged at 4000 rpm for 5 min and the upper layer was transferred to the sorbent (17 mg of

$\text{Fe}_3\text{O}_4@SiO_2@C18$ ) previously activated with methanol (2 mL), for 5 min. The mixture was vortexed for 1 min and then sonicated for 6 min. Subsequently, an ordinary magnet was placed at the bottom of the vial to harvest the  $\text{Fe}_3\text{O}_4@SiO_2@C18$  NPs and the supernatant was discarded. The EDCs were desorbed with 2.3 mL of *n*-hexane by ultrasonication (4 min) and the desorption solution was separated from the  $\text{Fe}_3\text{O}_4@SiO_2@C18$  NPs by the magnet and collected in a vial. The resulting solution was filtered through a 0.45  $\mu\text{m}$  membrane filter and the filtrates were evaporated to 50  $\mu\text{L}$ , under a gentle stream of nitrogen and transferred into amber vials for GC–MS analysis.

### 3. Results and discussion

#### 3.1. Characterization of sorbents

Characterizations of the synthesized MNPs ( $\text{Fe}_3\text{O}_4$ ,  $\text{Fe}_3\text{O}_4@SiO_2$  and  $\text{Fe}_3\text{O}_4@SiO_2@C18$ ) were performed, including SEM, XRD, EA, BET and FT-IR.

SEM revealed the nearly spherical shape of  $\text{Fe}_3\text{O}_4@SiO_2$  and  $\text{Fe}_3\text{O}_4@SiO_2@C18$  nanoparticles (Fig. 1).

FT-IR spectroscopy was employed to ensure proper chemical modification of the surface of MNPs. The band at  $570\text{ cm}^{-1}$  (Fig. 2a) represents the stretching vibration Fe–O–Fe of magnetite. The absorption peak at  $1068\text{ cm}^{-1}$  (Fig. 2b and c) can be attributed to the Si–O–Si vibration, while the peaks at  $1634$  and  $3400\text{ cm}^{-1}$  can be assigned to absorbed water or the silanol groups (Si–OH) of the silica. These peaks indicate the formation of a silica layer on the surface of  $\text{Fe}_3\text{O}_4$ . The characteristic peaks at  $2928$  and  $2854\text{ cm}^{-1}$  (Fig. 2c) differentiate the  $\text{Fe}_3\text{O}_4@SiO_2@C18$  NPs from  $\text{Fe}_3\text{O}_4@SiO_2$ . More specifically, they represent the asymmetric and the symmetric extension vibration of  $-\text{CH}_2-$  in the  $-(\text{CH}_2)_{17}\text{CH}_3$  chain, respectively, corroborating the introduction of  $-C18$  groups on the surface of the magnetite silica nanoparticles [34–37].

Elemental analysis of  $\text{Fe}_3\text{O}_4@SiO_2@C18$  NPs showed a carbon content of 7.05%. While the total specific surface area of  $\text{Fe}_3\text{O}_4@SiO_2@C18$  was found to be  $151\text{ m}^2/\text{g}$  using a BET plot.

Six characteristic peaks (Fig. 3) at  $2\theta$  of  $30.1^\circ$ ,  $35.5^\circ$ ,  $43.1^\circ$ ,  $53.4^\circ$ ,  $57.0^\circ$ , and  $62.6^\circ$ , identical to pure magnetite, occurred at XRD spectra of  $\text{Fe}_3\text{O}_4@SiO_2@C18$ , indicating that the functionalization of magnetite to form octadecylsilane nanoparticles does not cause a phase change in the cubic crystalline magnetite particles. The mean crystallite size ( $D$ , nm) of the particles was calculated using the

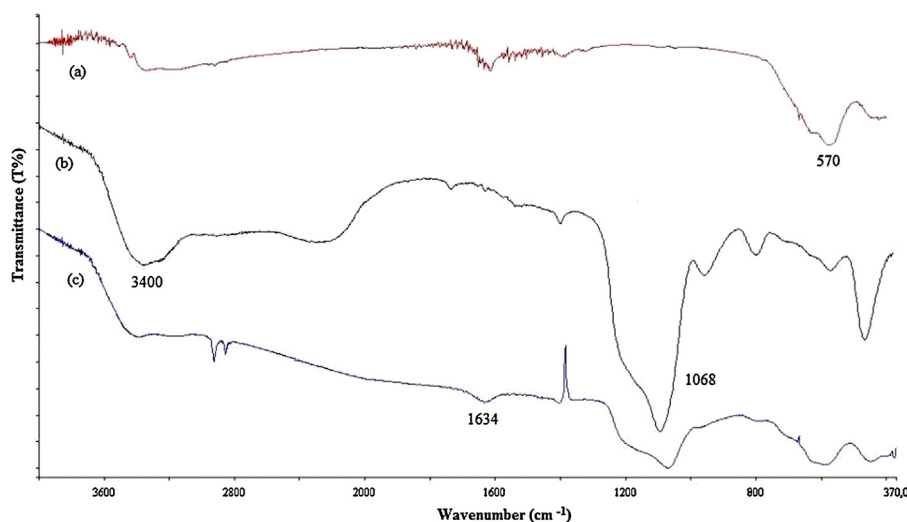


Fig. 2. FT-IR spectra of: (a)  $\text{Fe}_3\text{O}_4$ , (b)  $\text{Fe}_3\text{O}_4@SiO_2$  and (c)  $\text{Fe}_3\text{O}_4@SiO_2@C18$  magnetic nanoparticles (MNPs).

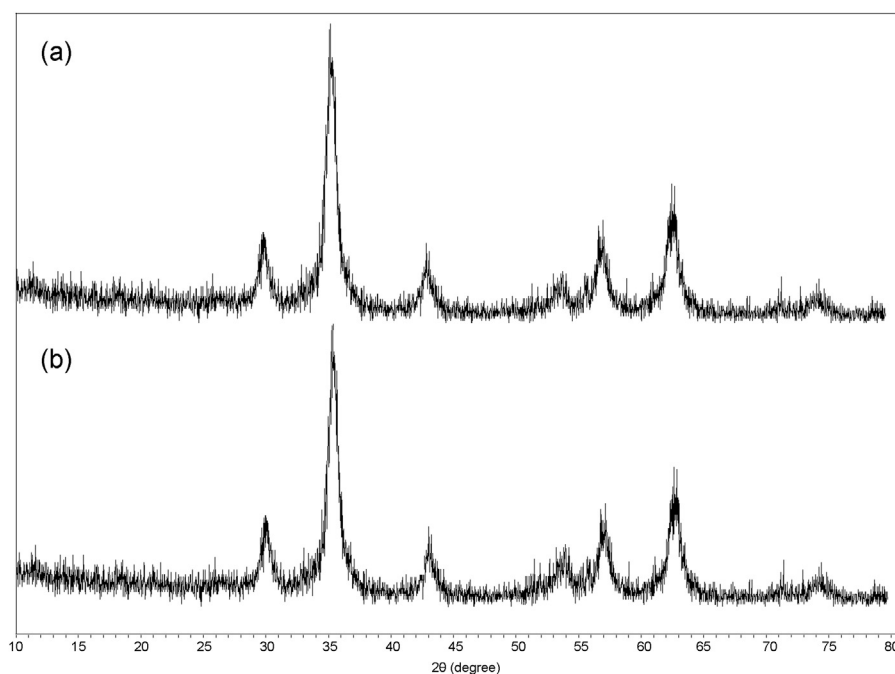


Fig. 3. XRD spectra of: (a)  $\text{Fe}_3\text{O}_4$  and (b)  $\text{Fe}_3\text{O}_4@\text{SiO}_2@\text{C18}$ .

Scherrer equation [38] and showed that the mean crystallite size of  $\text{Fe}_3\text{O}_4@\text{SiO}_2@\text{C18}$  is  $8.4 \pm 1.5$  nm.

### 3.2. Evaluation of sample pretreatment

In some cases, sample pretreatment via denaturation is employed prior to extraction, in order to release the target analytes from protein and/or to disrupt fat globules. To this end, sulphuric acid treatment is widespread [35]. Although certain OCPs are sensitive to acid treatment [15], most of the OCPs have been found to be relatively stable in the presence of a weak acid and therefore, formic acid (2 mL) was used in our study. Moreover, acetonitrile was added (125  $\mu\text{L}$ ) as it is hypothesized that disrupts the binding between the lipophilic OCPs and fat globules of milk [39]. Finally, aliquots of Carrez 1 (100  $\mu\text{L}$ ) and Carrez 2 (100  $\mu\text{L}$ ) were added to avoid turbid liquid and break any emulsions. The described sequence of pretreatment reduced the matrix effects (Fig. 4) – the Achilles heel of quantitative analysis – and yielded higher enrichment for the selected analytes. In the present study, besides sample pretreatment, matrix-matched calibration was also employed to combat matrix effects in GC–MS [40].

### 3.3. Optimization of the MSPE method

Preliminary experiments were performed in order to evaluate the efficiency of methanol, *n*-hexane and isooctane as eluting solvents. In all cases, prior to elution, MNPs were dried with a gentle stream of nitrogen. The results showed that the elution strength of *n*-hexane was much stronger than that of methanol and isooctane. Thus, *n*-hexane was selected as the elution solvent.

For the selection and assessment of the other main factors affecting the extraction profitability, a  $2^{7-4}$  screening design was applied followed by a Box–Behnken design for final optimization.

In this manner, variables such as the amount of sorbent ( $\text{Fe}_3\text{O}_4@\text{SiO}_2@\text{C18}$ ), the extraction and elution time, the sample volume, as well as the elution solvent (*n*-hexane) volume were studied in order to select the factors and the experimental domain that exhibit the highest extraction efficiency. Considering the multiresidue character of the proposed method, the mean recovery (*R* %) for all target analytes was selected as the depended variable (response, *Y*). The generation of the experimental design for screening and optimization, as well as the statistical evaluation of the results were performed by the STATISTICA 7.0 (StatSoft, Tulsa, OK, USA) statistical package.

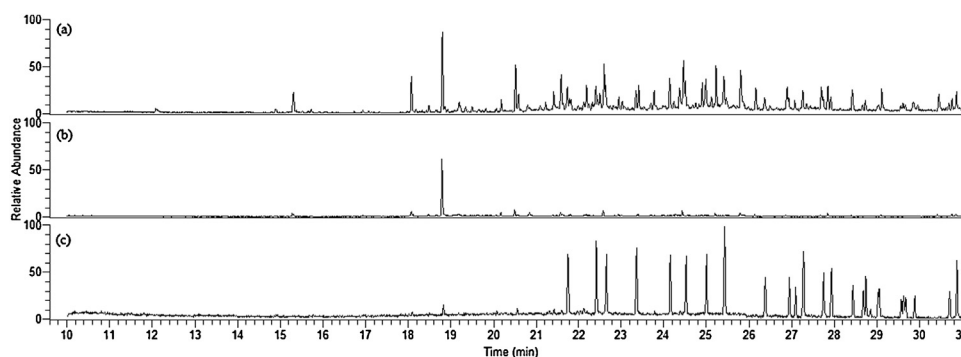


Fig. 4. MSPE–GC–MS chromatogram obtained from (a) a blank sample (without pretreatment), (b) a blank sample (after pretreatment), and (c) a spiked milk sample (100  $\mu\text{g}/\text{L}$ ) following the recommended procedure.



**Table 1**  
Box–Behnken design matrix of three variables in coded units and the response of average extraction efficiency (R %).

Factors	Levels					
	Low (-1)	Zero (0)	High (+1)			
(X <sub>2</sub> ) Sorbent amount (mg)				12	16	20
(X <sub>3</sub> ) <i>n</i> -Hexane volume (ml)				1.5	2	2.5
(X <sub>4</sub> ) Elution time (min)				4	5	6
Runs	X <sub>6</sub>	X <sub>4</sub>	X <sub>3</sub>	Average extraction efficiency (R %)		
1	1	1	0	86		
2	-1	-1	0	82		
3	0	0	0	52		
4	0	-1	1	51		
5	0	1	1	56		
6	0	-1	-1	55		
7	1	0	1	97		
8	1	-1	0	55		
9	0	0	0	124		
10	-1	0	1	86		
11	0	0	0	75		
12	-1	1	0	79		
13	-1	0	-1	108		
14	1	0	-1	69		
15	0	1	-1	113		

Analysis of variance (ANOVA) was performed to examine whether the studied experimental factors, were significant in the performance of the proposed method. An effect was considered significant when it was above the standard error, at the 95% confidence level ( $p < 0.05$ ). Sample volume was not significant ( $p = 0.10$ ), while for the remaining four significant variables a positive effect was observed for extraction time ( $p = 0.004$ ), sorbent amount ( $p = 0.005$ ) and *n*-hexane volume ( $p = 0.01$ ) and a negative effect was noticed for elution time ( $p = 0.03$ ).

### 3.3.1. Box-Behnken design (BBD)

Three-level-four-factor BBD [41] was used to optimize the extraction conditions for analyzing OPCs and PCBs in milk. Since extraction time (X<sub>1</sub>-Text), sorbent amount (X<sub>2</sub>-C18-NPs), *n*-hexane volume (X<sub>3</sub>-Vsolv) and elution time (X<sub>4</sub>-Telut), would significantly influence extraction efficiency, based on the outcome of the screening design, they were those variables to be chosen to optimize in order to achieve the highest extraction yield (Y, R %).

A total of 15 runs were carried out according to the BBD experimental design and low, middle and high levels of the coded values

were designated for the variables as 1, 0, and -1, respectively. The coded and actual levels of the independent variables in the BBD experimental design matrix are listed in Table 1.

Statistical analysis of variance (ANOVA) and regression model analysis were performed, and two-dimensional contour plots were drawn. It can be seen from pareto chart (Fig. 5), that two interaction coefficients (X<sub>3</sub>X<sub>4</sub>) and (X<sub>2</sub>X<sub>3</sub>) and one linear term coefficient (X<sub>2</sub>) were significant. Data analysis at 95% confidence level, permitted to obtain the following semi-empirical expression in terms of significant coded factors:

$$Y = 89.60 - 10.2X_2 + 14.4X_2X_3 - 17.2X_3X_4$$

where X<sub>2</sub> is the sorbent amount (C18-NPs), X<sub>3</sub> is the elution solvent volume (Vsolv) and X<sub>4</sub> is the elution time (Telut).

The model coefficient of determination ( $R^2 = 0.9600$ ) is in reasonable agreement with the experimental results. The adjusted determination coefficient (adjusted  $R^2 = 0.8881$ ) also advocates for a high significance of the model. Both values ensured a satisfactory correlation between the experimental and predicted values. Moreover, the lack of fit, which measures the failure of the model to

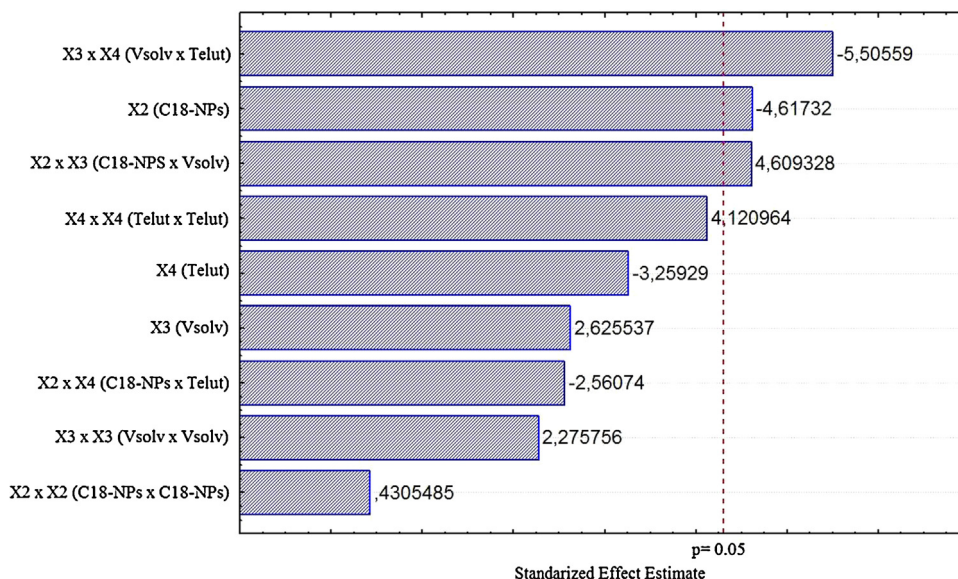


**Fig. 5.** Standardized main effect Pareto chart for the Box–Behnken design. Vertical line in the chart defines 95% confidence level.

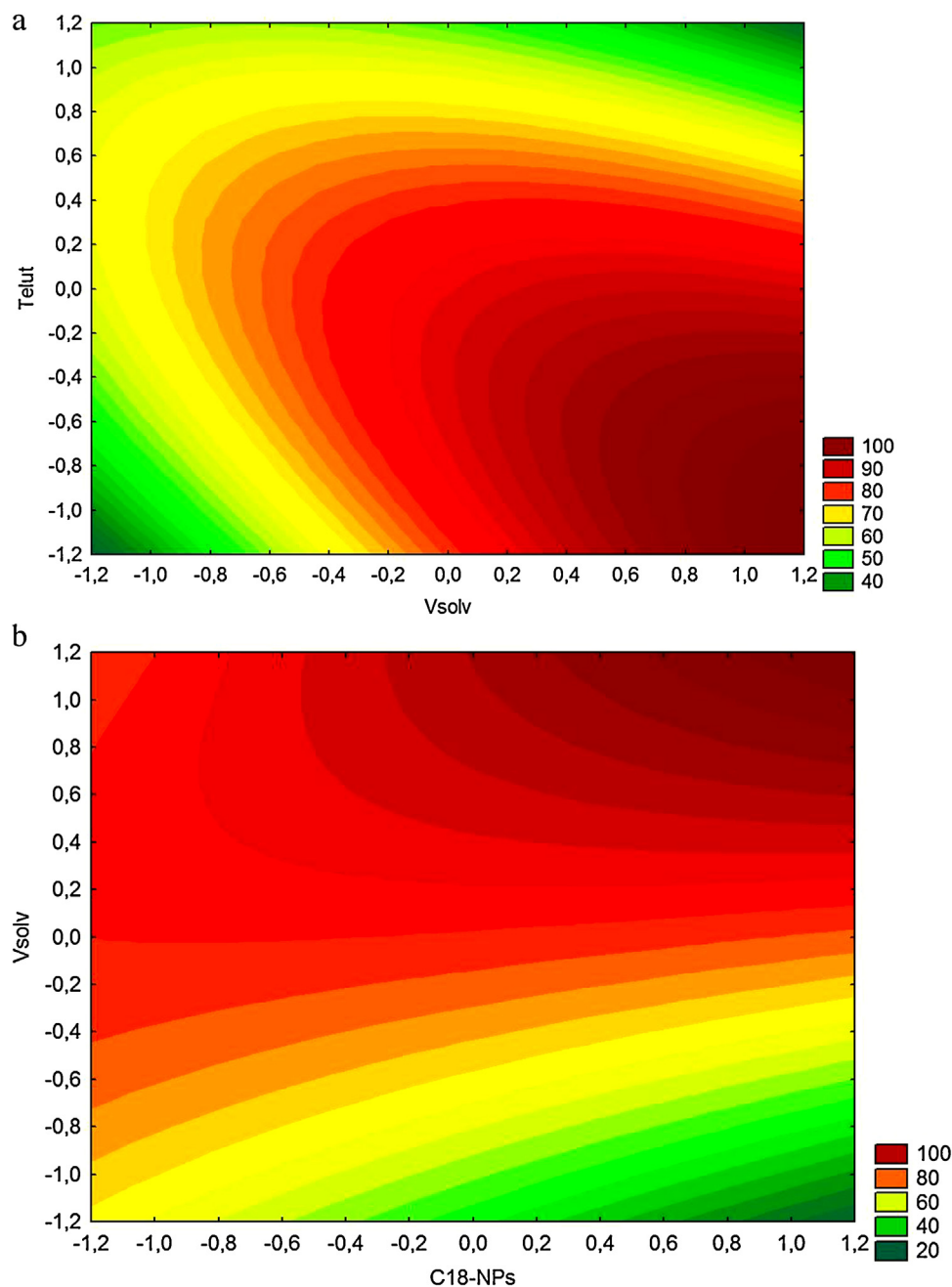


**Fig. 6.** Simulated two-parameter interaction–contour plots based on the Box–Behnken design. (a) Volume of elution solvent (*n*-hexane) vs elution time, (b) sorbent amount vs the elution solvent volume. Z-axis depicts the extraction efficiency expressed as average recovery for all target analytes (R%).

represent data in the experimental domain at points which are not included in the regression, showed to be non-significant ( $p=0.54$ ) relative to the pure error, indicating a good response to the model.

On the basis of results of the BBD, two 2D contour plots are illustrated in Fig. 6, which portray the interaction effects between the volume of elution solvent (*n*-hexane) and the elution time (Fig. 6a) and between the sorbent amount and the elution solvent volume (Fig. 6b). When low amounts of *n*-hexane are introduced (Fig. 6a), the extraction efficiency declines irrespectively of the contact time between *n*-hexane and  $\text{Fe}_3\text{O}_4@/\text{SiO}_2@/\text{C18}$  (elution time). Higher yields were obtained when higher amounts of sorbent were used for the extraction. The reflected interaction effects between sorbent amount and *n*-hexane volume (Fig. 6b), demonstrated that the

highest recovery of the target analytes was observed at the highest values of both variables.

Finally, optimal extraction conditions were obtained using the desirability function of the statistical software. The optimal conditions to extract EDCs from milk samples with the aid of MSPE were: 17 mg of  $\text{Fe}_3\text{O}_4@/\text{SiO}_2@/\text{C18}$  as sorbent and 2.3 mL *n*-hexane as elution solvent, for an elution time of 4 min. Under optimal conditions, the model predicted maximum total extraction profitability of 97%. In order to verify the accuracy of the model, three additional experiments were conducted, under optimal conditions. The experimental average recovery obtained was 93%, which was in good agreement with the predictive value, indicating the adequacy of the response model for the extraction process.

**Table 2**  
Validation parameters obtained for EDCs after MSPE and GC/MS. Accuracy—R (%), intra-day precision—RSDr (%), within-lab reproducibility RSD<sub>WR</sub> (%) on fortification levels equal to LOQs and MRLs.

	Fortification level at LOQ			Fortification level at MRL			LOD (μg/L)	LOQ (μg/L)
	Rec (%)	RSDr (%)	RSD <sub>WR</sub> (%)	Rec(%)	RSDr (%)	RSD <sub>WR</sub> (%)		
a-BHC	98	4	8	99	4	11	0.3	0.9
b-BHC	95	4	5	89	3	6	0.2	0.8
γ-BHC	79	10	12	84	10	12	0.1	0.4
δ-BHC	93	4	9	96	5	7	0.3	0.9
PCB 28	91	5	6	86	5	6	0.1	0.2
Heptachlor	91	4	5	92	4	7	0.1	0.2
PCB 52	92	4	5	96	2	5	0.1	0.3
Aldrin	94	6	7	98	6	7	0.1	0.3
Heptachlor epoxide	100	7	11	88	7	13	0.1	0.2
γ-chlordane	89	5	8	90	6	8	0.1	0.3
PCB 101	94	3	3	95	3	7	0.1	0.4
a-chlordane	94	3	4	96	4	4	0.1	0.2
endosulfan I	101	5	8	88	5	9	0.1	0.2
p,p'-DDE	90	6	8	82	6	8	0.1	0.4
Dieldrin	91	8	11	96	9	13	0.1	0.4
Endrin	103	10	11	116	10	11	0.1	0.2
Endosulfan II	97	2	4	104	3	6	0.3	1
p,p'-DDD	82	12	14	82	12	14	0.1	0.5
Endrin aldehyde	107	4	6	95	4	6	0.2	0.8
PCB 153	91	4	5	87	6	8	0.1	0.3
Endosulfan sulfate	82	5	5	84	5	5	0.1	0.3
p,p'-DDT	81	4	6	87	4	10	0.2	0.7
PCB 138	102	4	7	101	5	7	0.1	0.3
Endrin ketone	96	4	8	99	3	8	0.3	1
Methoxychlor	96	5	9	93	8	11	0.1	0.5
PCB180	92	7	8	98	5	8	0.1	0.3

### 3.4. Analytical performance and method validation

The optimum conditions were implemented to verify the applicability of the proposed method for the quantitative determination of target analytes. The validation scheme followed was based on the SANCO/12571/2013 European Guidelines [42]. Quality parameters including the specificity, the linear range, the repeatability (RSDr), the within-laboratory reproducibility (RSD<sub>WR</sub>), the accuracy, the limits of detection (LODs), and limits of quantification (LOQs) were investigated.

#### 3.4.1. Specificity

The specificity of the method was tested by the analysis of blank samples. The absence, in every matrix, of any chromatographic peak at retention times where the target pesticides elute, indicated that there were no matrix effects which might give a false positive signal in these blank samples.

#### 3.4.2. Linear range

Calibration curves were established applying the method of standard additions: the samples were fortified with known amounts of analytes before sample preparation with the LOQs to be the lowest levels for each analyte. This calibration method was selected in order to compensate for potential matrix effects occurring during sample preparation and analysis. The calculated calibration curves (seven points, each calibration point was determined in triplicate) gave a high level of linearity for all target analytes with coefficients of determination ( $R^2$ ) ranging between 0.9950 and 0.9999. Moreover, residual plots were prepared for each analyte. Individual residuals were scattered randomly above and below zero, with standard deviations ranging from 0.33% to 7.5%, lower than  $\pm 20\%$  ( $\pm 10\%$  when the Maximum Residue Limit—MRL is approached or exceeded) from the calibration curve, as suggested by SANCO/12571/2013 document.

#### 3.4.3. Accuracy and precision

The accuracy and precision of the developed method were assessed at three different concentration levels, corresponding to LOQ, MRL and five times the MRL limits for each compound. Accuracy is expressed as analyte recovery ( $R\%$ ) i.e. percent closeness between the calculated and the theoretical concentrations of the spiked milk samples for each analyte, whereas intraday precision, or within-lab reproducibility, was calculated as the percent relative standard deviation (RSD %) of five replicates (Table 2). Recoveries ranged from 79% to 116%, while the calculated RSDr and RSD<sub>WR</sub> ranged from 2% to 12% and from 4% to 14%, respectively, complying with the requirements of SANCO document ( $R\% 70\text{--}120\%$ , RSDr, RSD<sub>WR</sub>  $\leq 20\%$ ).

#### 3.4.4. Limits of detection and limits of quantification

The LODs and LOQs for all target analytes were calculated according to the criteria of signal-to-noise = 3 and signal-to-noise = 10, respectively. Both LODs and LOQs are presented in Table 2. Although these terms usually refer to the method's limits, in this case the reported values represent the LODs and LOQs of the method taking into account the relevant matrix effects. The calculated LODs and LOQs are acceptable, exhibiting compliance with the MRLs established by European Commission [17] and Codex Alimentarius Commission [43], for OCPs and PCBs residues in milk.

#### 3.5. Reusability of Fe<sub>3</sub>O<sub>4</sub>@SiO<sub>2</sub>@C18 nanosorbent

The reusability of Fe<sub>3</sub>O<sub>4</sub>@SiO<sub>2</sub>@C18 magnetic sorbents for the extraction of target analytes was also investigated. The magnetic sorbent was regenerated by washing twice with acetone, after each adsorption–elution cycle. In such way, no carry-over of the analytes on the adsorbent was detected. The recoveries of OCPs and PCBs and hence the extraction capacity of the remained constant after three successive cycles, indicating good stability and reusability. After three cycles a gradual loss of the extraction efficiency was observed for all target analytes.



### 3.6. Application to real samples

To demonstrate the applicability of MSPE for routine analysis, the described method was applied to the determination of EDCs in five semi-skimmed milk samples obtained from local markets. The results revealed that the selected milk samples were free from contamination from the target analytes.

In order to evaluate the accuracy of MSPE, blank milk samples were fortified at a concentration level of 5 µg/L and analyzed by the proposed method, as well as by a solid-phase microextraction (SPME) adopted by Fernandez-Alvarez et al. [17]. Application of paired *t*-test at 95% confidence level showed that no significant difference was observed between the two methods.

## 4. Conclusions

Functionalized MNPs were synthesized to serve as solid-phase extraction sorbents for simultaneous enrichment and detection of endocrine disrupting compounds in milk samples with the aid of GC–MS. Analyte extraction and desorption were carried out quickly and the whole pretreatment process could be accomplished by simple vortex and ultrasonication within 25 min. The applicability, accuracy, precision, sensitivity of the proposed method have been demonstrated based on SANCO/12571/2013 European Guidelines. LODs were below the MRLs set by the European Union for all compounds studied. Considering that Fe<sub>3</sub>O<sub>4</sub>@SiO<sub>2</sub>@C18 nanoparticles inherit the virtues of being easy-to-prepare, cost-effectiveness and ease of separation and dispersion, this protocol is believed to be promising for the screening of the selected compounds in milk matrices.

## Acknowledgments

This research project has been co-financed by the European Union (European Regional Development Fund-ERDF) (MIS: 348148) and Greek national funds through the Operational Program “THESSALY-MAINLAND GREECE AND EPIRUS-2007–2013” of the National Strategic Reference Framework (NSRF 2007–2013).

The use of the XRD and SEM units of the Network of Research Units of the University of Ioannina and especially Dr. Papachristodoulou and Dr. Tsaousi is gratefully acknowledged. Many thanks are due to Assist. Prof. D. Petrakis for the N<sub>2</sub> adsorption–desorption porosimetry measurements.

## References

- [1] Environmental Protection Agency, Draft list of initial pesticide active ingredients and pesticide inerts to be considered for screening under the federal food, drug, and cosmetic act, in: Federal Register, 72, Environmental Protection Agency, 2007, Notices.
- [2] Q. Li, M.H.W. Lam, R.S.S. Wu, B. Jiang, J. Chromatogr. A 1217 (2010) 1219.
- [3] V.I. Boti, V.A. Sakkas, T.A. Albanis, J. Chromatogr. A 1216 (2009) 1296.
- [4] V.I. Boti, V.A. Sakkas, T.A. Albanis, J. Chromatogr. A 1146 (2007) 139.
- [5] Pesticide Action Network UK, The List of Lists (2005), <http://www.pan-uk.org>.
- [6] G.N. Rallis, V.A. Sakkas, V.A. Boumba, T. Vougiouklakis, T.A. Albanis, J. Chromatogr. A 1227 (2012) 1.
- [7] H.R. Norli, A. Christiansen, E. Deribe, J. Chromatogr. A 1218 (2011) 7234.
- [8] A. Derouichea, M.R. Drissa, J.-P. Morizurb, M.-H. Taphanel, J. Chromatogr. A 1138 (2007) 231.
- [9] M. LeDoux, J. Chromatogr. A 1218 (2011) 1021.
- [10] S.M. Goulart, M.E.L.R. de Queiros, A.A. Neves, J.H. de Queiros, Talanta 75 (2008) 1320.
- [11] A. Di Muccio, P. Pelosi, D. Attard Barbini, T. Generali, A. Ausili, F. Vergori, J. Chromatogr. A 765 (1997) 51.
- [12] S. Bogianni, R. Curini, A. Di Cortia, A. Lagana, M. Nazzari, M. Tonci, J. Chromatogr. A 1054 (2004) 351.
- [13] E. Kampire, B.T. Kiremire, S.A. Nyanzi, M. Kishimba, Chemosphere 84 (2011) 923.
- [14] S.M. Waliszewski, V.T. Pardío, K.N. Waliszewski, J.N. Chantiri, A.A. Aguirre, R.M. Infanzón, J. Rivera, Sci. Total Environ. 208 (1997) 127.
- [15] J.G. Martins, A.A. Chavez, S.M. Waliszewski, A.C. Cruz, M.M. García Fabila, Chemosphere 92 (2013) 233.
- [16] L. Kantiani, M. Farré, M. Sibum, C. Postigo, M. López de Alda, D. Barceló, Anal. Chem. 81 (2009) 4285.
- [17] M. Fernandez-Alvarez, M. Llompart, J.P. Lamas, M. Lores, C. Garcia-Jares, R. Cela, T. Dagnac, Anal. Chim. Acta 617 (2008) 37.
- [18] T. Dagnac, M. Garcia-Chao, P. Pulleiro, C. Garcia-Jares, M. Llompart, J. Chromatogr. A 1216 (2009) 3702.
- [19] I.S. Jeong, B.M. Kwak, J.H. Ahn, S.H. Jeong, Food Chem. 133 (2012) 473.
- [20] A. Ashnagar, N.G. Naseri, M.C. Farmad, Int. J. Pharm. Tech. Res. 1 (2) (2009) 247.
- [21] C.H.P. Ciscato, A.B. Gebara, H.S. Spinosa, J. Environ. Sci. Health, B 37 (4) (2002) 323.
- [22] S. Bulut, L. Akkaya, V. Gok, M. Konuk, Environ. Monit. Assess. 181 (2011) 555.
- [23] O.P. Luzardo, M. Almeida-González, L.A. Henríquez-Hernández, M. Zumbado, E.E. Alvarez-León, L.D. Boada, Chemosphere 88 (2012) 307.
- [24] S. Ghidini, E. Zanardi, A. Battaglia, G. Varisco, E. Ferretti, G. Campanini, R. Chizzolini, Food Addit. Contam. 22 (1) (2005) 9.
- [25] D. Lambropoulou, T. Albanis, Anal. Bioanal. Chem. 389 (2007) 1663.
- [26] N.C. Maragou, E.N. Lampi, N.S. Thomaidis, M.A. Koupparis, J. Chromatogr. A 1129 (2006) 165.
- [27] Q. Gao, D. Luo, J. Ding, Y.Q. Feng, J. Chromatogr. A 1217 (2010) 5602.
- [28] R. Lucena, B.M. Simonet, S. Cárdenas, M. Valcárcel, J. Chromatogr. A 1218 (2011) 620.
- [29] X.S. Li, G.T. Zhu, Y.B. Luo, B.F. Yuan, Y.Q. Feng, Trends Anal. Chem. 45 (2013) 233.
- [30] C. Jiang, Y. Sun, X. Yu, Y. Gao, L. Zhang, Y. Wang, H. Zhang, D. Song, J. Chromatogr. B 947–948 (2014) 49.
- [31] Y. Zhang, M. Kuang, L. Zhang, P. Yang, H. Lu, Anal. Chem. 85 (2013) 5535.
- [32] J.E. Smith, L. Wang, W. Tan, Trends Anal. Chem. 25 (9) (2006) 841.
- [33] E. Tahmasebi, Y. Yamini, M. Moradi, A. Esrafil, Anal. Chim. Acta 770 (2013) 68.
- [34] B. Maddah, J. Shamsi, J. Chromatogr. A 1256 (2012) 40.
- [35] A. Covaci, C. Hura, R. Schepens, Chromatographia 54 (2001) 247.
- [36] Y.X. Liu, G.Q. Jian, X.W. He, L.X. Chen, Y.K. Zhang, Chin. J. Anal. Chem. 41 (2) (2013) 161.
- [37] S. Zhang, H. Niu, Y. Zhang, J. Liu, Y. Shi, X. Zhang, Y. Cai, J. Chromatogr. A 1238 (2012) 38.
- [38] M. Morel, F. Martínez, E. Mosquera, J. Magn. Mater. 343 (2013) 76.
- [39] S.W.C. Chung, B.L.S. Chen, J. Chromatogr. A 1218 (2011) 5555.
- [40] H. Kwon, S.J. Lehotay, L. Geis-Asteggiane, J. Chromatogr. A 1270 (2012) 235.
- [41] C. Stalikas, Y. Fiamegos, V. Sakkas, T. Albanis, J. Chromatogr. A 1216 (2009) 175.
- [42] European Commission Health & Consumer protection Directorate-General, Guidance document on analytical quality control and validation procedures for pesticide residues analysis in food and feed, in: SANCO/12571/2013, European Commission Health & Consumer protection Directorate-General, November 2013.
- [43] Codex Alimentarius Commission, International Food Standards, URL: <http://www.codexalimentarius.org>.